Journal of Alloys and Compounds 531 (2012) 82–85

Contents lists available at SciVerse ScienceDirect

Journal of Alloys and Compounds

journal homepage: www.elsevier.com/locate/jallcom

Electronic structure and impurity states of S-doped cBN: A first-principle study

Y.B. Li[a], H.X. Jiang[a], G.Z. Yuan[b], A.L. Chen[b], X. Wang[a], T.G. Dai[a], H.S. Yang[b,*]

[a] Institute of Microelectronics and Optoelectronics, Department of Information Science and Electronic Engineering, Zhejiang University, Hangzhou 310027, China
[b] State Key Laboratory of Silicon Materials, Department of Materials Science and Engineering, Zhejiang University, Hangzhou 310027, China

ARTICLE INFO

Article history:
Received 13 February 2012
Received in revised form 22 March 2012
Accepted 1 April 2012
Available online 10 April 2012

Keywords:
Cubic boron nitride
Sulfur
Doping
Bandgap
First-principle study

ABSTRACT

The electronic structure and impurity states of S-doped *c*BN were investigated by first-principle approaches. Our calculation shows that S substituted for an N atom creates shallow donor levels merged to the states at the conduction band edge, S substituted for a B atom creates deep donor levels within the band gap, both forming n-type cBN, and band gap of S-doped *c*BN decreases with the increase of dopant concentration. Moreover, from the view of energy, S is more likely to be substituted for a B atom than an N atom.

1. Introduction

Cubic boron nitride (cBN) is currently attracting considerable interest for applications in the fields of high-temperature and high-power electronic devices because of its excellent chemical stability, high thermal conductivity, wide bandgap with both n- and p-type dopability and a large breakdown electric field [1]. However, due to the difficulty of growing high quality cBN films and large size cBN single crystals, there are still few groups in number that can make high quality cubic phase boron nitride [2–9], let alone high quality n- or p-type doped cBN that can be used to fabricate excellent performance electronic devices. In the experimental aspect, Taniguchi et al. [10–13], one of the famous groups that have synthesized large size cBN single crystals successfully, reported various characteristics of n- and p-type cBN single crystal doped with S, Be, Eu and Tb. Electrical properties of Be-implanted polycrystalline cBN films were also studied by He et al. [14]. Yoshida and Nose et al., reported semiconducting properties of Mg- and Zn-doped cBN thin films [15–17]. Recently, electrical transport properties of Si-doped cBN thin films were reported by Ying et al. [18]. In the theoretical aspect, vacancies of boron (B) and nitrogen (N), impurity of Be, Mg and Si in cBN have been studied by Gubanov et al. [19,20]. A systematic review of first-principle calculations for defect and impurities to III-nitrides but mainly to GaN was presented by Van de Walle and Neugebauer [21]. As we can see, the characteristics of S-doped cBN still remain a rare studied problem that is worth investigating in both theory and experiment.

In this work, we present first-principle investigations on the electronic structure and impurity states of substitutional S-doped cBN. The results of S substituting a nitrogen atom are compared with those of substituting a boron atom. Effects of different doping concentrations on the electronic structure are also discussed. Our calculations suggest that S is easier to substitute a B atom than an N atom, and S substitution at an N atom will induce shallow level near the bottom of conduction band minimum, while S substitution at a B atom will induce deep levels within the band gap.

2. Method of calculations

To find the sulfur impurity states and its influence on the intrinsic host cBN crystal, total energy and electronic structure of S-doped cBN were investigated within density functional theory (DFT) as implemented in the Cambridge Sequential Total Energy Package (CASTEP) code [22], using exchange-correlation functional in the CA-PZ form [23,24] of local density approximation (LDA). A plane wave basis set expanded to an energy cutoff of 100 Ry and ultrasoft pseudopotential depicting the interactions between valence electrons and the ionic core were used to describe the electronic wave functions with integration over the Brillouin zone by summation over a $20 \times 20 \times 20$ Monkhorst-Pack k-point mesh. In addition, the valence atomic configurations were used as $2s^2 2p^1$, $2s^2 2p^3$, and $3s^2 3p^4$ for B, N and S, respectively. In order to study the effects of different concentrations of impurity on the properties of cBN, 32-, 64-, 96- and 128-atom supercell models were used with one

* Corresponding author. Tel.: +86 571 87951404; fax: +86 571 87951411.
E-mail address: hsyang@zju.edu.cn (H.S. Yang).

0925-8388/$ – see front matter © 2012 Elsevier B.V. All rights reserved.
http://dx.doi.org/10.1016/j.jallcom.2012.04.002

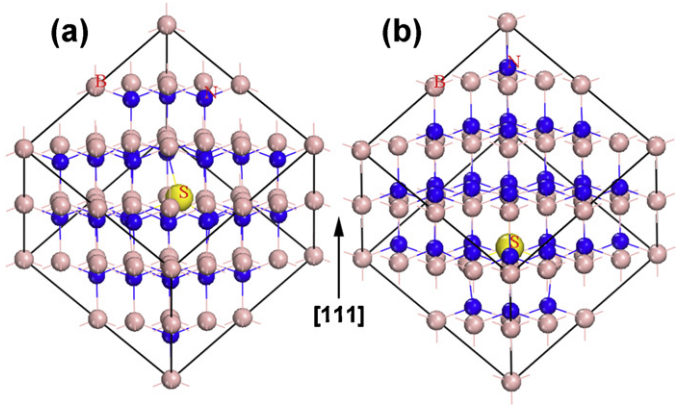

Fig. 1. 64-Atom supercell structure (a) S substitution at the B site; (b) S substitution at the N site. Pink ball: B; blue ball: N; yellow ball: S.

sulfur atom substitution at the center or near center of each supercell, yielding an effective impurity concentration of 3.13%, 1.56%, 1.04% and 0.78%, respectively. All atomic coordinates were relaxed and the structure optimization was performed until the energy change of per atom was less than 1.0×10^{-5} eV, the Hellmann–Feynman forces on atoms were less than 0.03 eV/Å, and the maximum displacement of per atom was 1.0×10^{-3} Å. Note that the scissor operation of 1.9 eV [25,26], a linear shift of the calculated band structure, has been used to correct the theoretical bandgap compared with the widely admitted experimental value, due to the well-known underestimation to all of the LDA calculations in which the correlation energy of excited electrons is ignored. Another theoretical investigation using the general gradient approximation (GGA) was also performed to check the accuracy, and the lattice parameters and band gap of pure cBN agree well with each other (shown in Table 1) and previous experimental results [27].

3. Results and discussion

Supercell structure of sulfur impurity substitutions at a B atom and an N atom (taking a 64-atom supercell as an example) are shown in Fig. 1. Total energy values of different supercell sizes are shown in Fig. 2a, and we can see that the total energy of S substitution at the B site is less than that of S substitution at the N site, which means that S substituting at the B site is easier and structural stable. This calculation result is consistent with our previous experiment [28]. As shown in Fig. 2b, for a cBN film prepared by PECVD with the introduction of H_2S into the deposition system, the increase of S second ion intensity measured from the depth profile second ions mass spectroscopy (SIMS) of the S-doped cBN was accompanied with a decrease of B second ion intensity, suggesting that S is mainly substituted for B atom. Fig. 2a also shows that the total energy difference between S atom substitution at the N site and at the B site is independent on the supercell sizes, remaining about 190 eV. This mainly results from that the difference of formation energy between S substitution at the B and N site with same cell size is a constant where influence of supercell size is minimized.

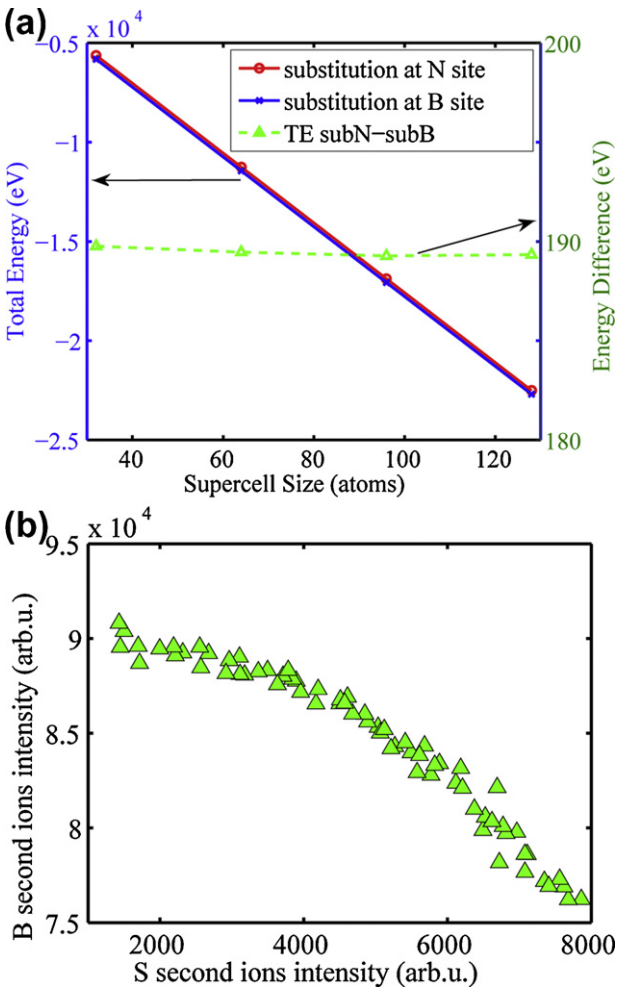

Fig. 2. (a) Total energy of varying cBN supercell size and energy difference between S substitution at the B and N site. The total energy of S substitution at the B site is about 190 eV less than that of S substitution at the N site with the same supercell size. (b) Second ions intensity of S and B in an S-doped cBN film measured by depth profile SIMS. S-doped cBN films were prepared by PECVD.

The calculation of energy band structure of ideal intrinsic cBN indicates that pure cBN is indirect bandgap semiconductor material with a minimum bandgap of ~6.29 eV between G and X in the reciprocal space (shown in the inset of Fig. 3a and Table 1), consistent with previous results [27,29]. The energy band of S-doped cBN is much complicated, mainly due to impurity atoms inducing energy levels of hybrid orbitals when forming S—B bonds or S—N bonds. Total electron density of states (DOS) for cBN with different S-doping levels presented in Fig. 3 indicates the details of band structure variation with sulfur concentration. We note that the bandgap decreases as the impurity concentration increases. The calculated bandgap is 5.41, 5.35, 5.25 and 4.95 eV for S substitution at the N site with doping concentration of 0.78%, 1.04%, 1.56% and 3.13%, respectively. For S substitution at the B site, the calculated bandgap is 5.62, 5.55, 5.03 and 4.63 eV (shown in the inset

Table 1
Geometry optimized structural parameters and band gap of pure cBN comparing with GGA approach and experimental results.

	This work		Literature [27]
	LDA/CA-PZ	GGA/PBE	
a (Å)	3.588	3.638	3.615
B—N bond length (Å)	1.554	1.575	1.570
Band gap (eV) (scissor = 1.9 eV)	4.39 + 1.9 = 6.29	4.44 + 1.9 = 6.34	6.1–6.4

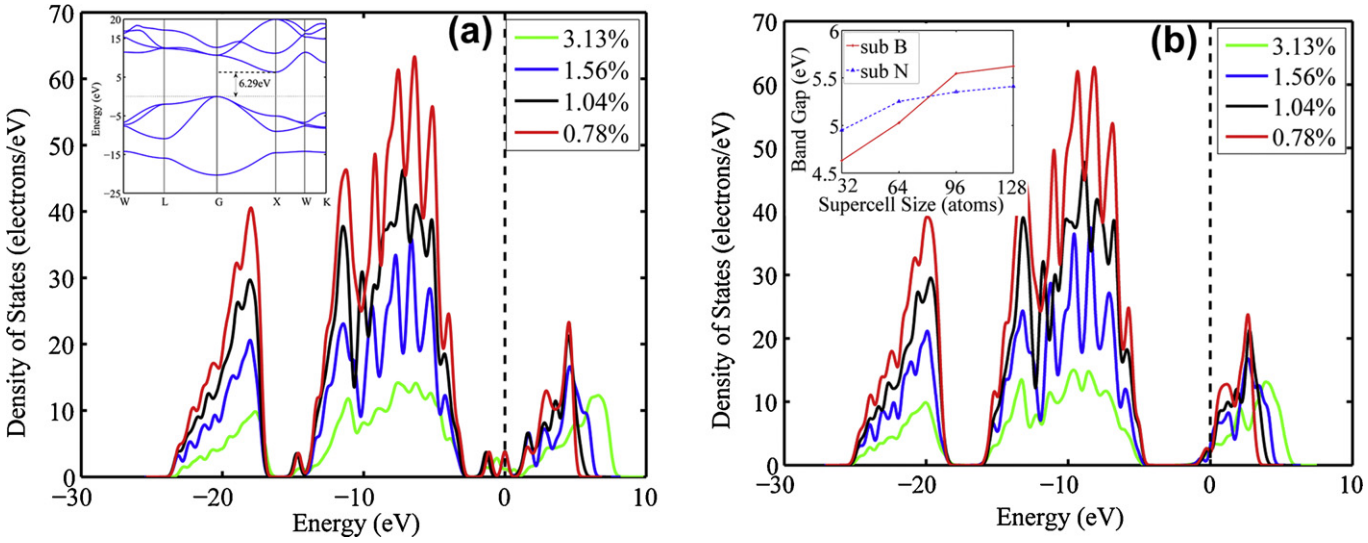

Fig. 3. Density of states of different S-doping level cBN. (a) S substitution at the B site (inset is the calculated energy band scheme of pure cBN). (b) S substitution at the N site (inset is the relationship between band gap and supercell size).

of Fig. 3b). As analyzed in the following section, this might result from that one of the S 3p orbitals which is near the conduction band hybridizes with B 2p orbital.

To further investigate contributions of different atom species to the energy level, partial density of states (PDOS) of S-doped cBN is displayed in Fig. 4. When S substituted at the B site, S 3s orbital overlap with its neighboring nitrogen 2s and 2p orbital, forming one peak at the bottom of upper valance band (about −14.7 eV), and two of the S 3p orbitals hybridize with N 2p orbital, resulting in deep energy levels within the band gap (about −1.3 eV and 0 eV); another S 3p orbital hybridizes with its neighboring N 2p orbital, forming peaks at the conduction band (shown in Fig. 4a and c). While for S substitutes at the N site, S 3s orbital hybridizes with its neighboring B 2s and 2p orbital forming peak at the top of lower valance band; two of the S 3p orbitals forming bond with B 2p, forming peaks at the bottom of upper valance band, and another S 3p orbital hybridizes with its neighboring B 2p orbitals, forming peaks at the conduction band (shown in Fig. 4b and d). The PDOS analysis shows that the substitutional S atom induces certain impurity states within the bandgap and near band edge of pure cBN bulk, resulting in the bandgap reduction from 6.3 eV of pure cBN to 4.6 eV and 5.0 eV (3.13% impurity concentration) of S doped at the

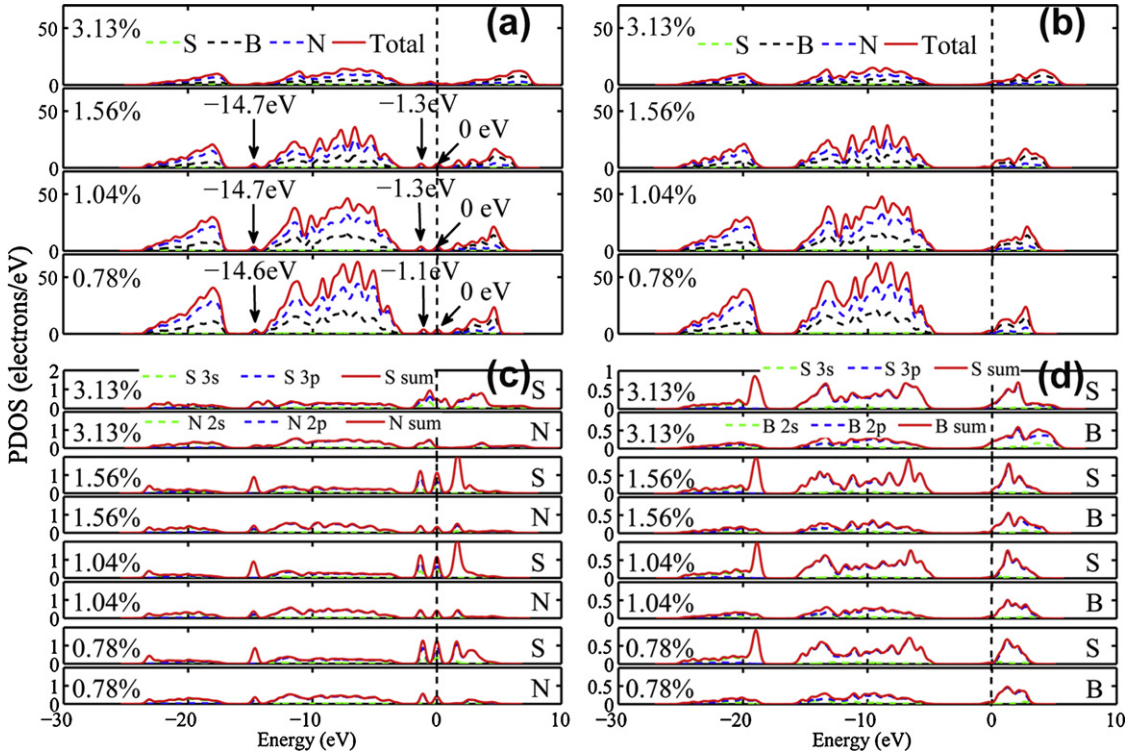

Fig. 4. Partial density of states of S-doped cBN with different doping levels (a) contributions of different elements where S substitutes at the B site, (b) contributions of different elements where S substitution at the N site, (c) PDOS of S atom and its neighboring N atom where S substitutes at the B site, and (d) PDOS of S atom and its neighboring B atom where S substitutes at the N site.

B and N site, respectively. Particularly, when S substitutes at the B site with a doping level of 3.13%, the PDOS of S atom shows that electron states have almost occupied within the whole bandgap, which is different from the PDOS of the other three doping levels. In the three less S-content levels, S induced discrete energy levels in the bandgap. The reason might be that 3.13% S-doping level is high that the doped cBN crystal has become degenerate. As a result, the S atom substitution at the B site induces deep impurity level, while the S atom substitution at the N site induces shallow level within the band gap. The greater negative total energy in the case of S substitution for B (S → B) than for N (S → N) shown in Fig. 2 suggests that bond energy of S(S → B)—N is stronger and more stable than that of S(S → N)—B. This can be explained by the number of valance electrons of an S atom. That is, S(S → N) and S(S → B) have one or three more valance electrons than the original N or B atoms in the unperturbed lattice, respectively. On the other hand, electron state of S(S → B) is less localized than that of S(S → N) due to closer electron affinity between S and N than the case between S and B bonds. It means that higher transition probability for carriers is expected in the case of S substitution at a B atom. The calculations discussed above suggest that S substitutional impurities can create electron states near the bottom of the conduction band and within the band gap, which can result in n-type conductivity in S-doped cBN.

4. Conclusions

In summary, we have performed first principle calculations to investigate the electronic structure and impurity states of S-doped cBN with different doping concentration. Bandgap of S-doped cBN decreases with the increase of S content in the host crystal. S substitution at an N site will induce shallow level near the bottom of conduction band, and S substitution at a B site will induce deep levels within the band gap, both resulting in n-type cBN. Both the theoretical and experimental results show that S is apt to be doped at a B site.

Acknowledgements

We want to thank Prof. Y. Liu from Dept. of Mater. Sci. & Eng. at Zhejiang Univ. for his helpful discussion with us. This work was financially supported by the National Natural Science Foundation of China (No. 61176051 and 50772096).

References

[1] S. Noor Mohammad, Electrical characteristics of thin film cubic boron nitride, Solid-State Electronics 46 (2002) 203–222.
[2] W.J. Zhang, Y.M. Chong, I. Bello, S.T. Lee, Nucleation, growth and characterization of cubic boron nitride (cBN) films, Journal of Physics D: Applied Physics 40 (2007) 6159.
[3] S. Matsumoto, W. Zhang, High-rate deposition of high-quality, thick cubic boron nitride films by bias-assisted DC jet plasma chemical vapor deposition, Japan Journal of Applied Physics 39 (2000) 442.
[4] H. Yang, C. Iwamoto, T. Yoshida, High-quality cBN thin films prepared by plasma chemical vapor deposition with time-dependent biasing technique, Thin Solid Films 407 (2002) 67–71.
[5] X.W. Zhang, H.G. Boyen, N. Deyneka, P. Ziemann, F. Banhart, M. Schreck, Epitaxy of cubic boron nitride on (0 0 1)-oriented diamond, Nature Materials 2 (2003) 312–315.
[6] H. Yang, C. Iwamoto, T. Yoshida, Interface engineering of cBN films deposited on silicon substrates, Journal of Applied Physics 94 (2003) 1248–1251.
[7] W. Zhang, I. Bello, Y. Lifshitz, K.M. Chan, X. Meng, Y. Wu, C.Y. Chan, S.T. Lee, Epitaxy on diamond by chemical vapor deposition: a route to high-quality cubic boron nitride for electronic applications, Advanced Materials 16 (2004) 1405–1408.
[8] H. Yang, C. Iwamoto, T. Yoshida, Direct nucleation of cubic boron nitride on silicon substrate, Diamond and Related Materials 16 (2007) 642–644.
[9] H. Yang, A. Chen, F. Qiu, Cubic boron nitride film residual compressive stress relaxation by post annealing, Diamond and Related Materials 20 (2011) 1179–1182.
[10] T. Taniguchi, K. Watanabe, S. Koizumi, I. Sakaguchi, T. Sekiguchi, S. Yamaoka, Ultraviolet light emission from self-organized p–n domains in cubic boron nitride bulk single crystals grown under high pressure, Applied Physics Letters 81 (2002) 4145–4147.
[11] T. Taniguchi, T. Teraji, S. Koizumi, K. Watanabe, S. Yamaoka, Appearance of n-type semiconducting properties of cBN single crystals grown at high pressure, Japan Journal of Applied Physics 41 (2002) 109.
[12] K. Watanabe, T. Taniguchi, H. Kanda, E.M. Shishonok, Polarized Raman scattering of impurity modes in beryllium-doped cubic boron nitride single crystals, Applied Physics Letters 82 (2003) 2972–2974.
[13] A. Nakayama, T. Taniguchi, Y. Kubota, K. Watanabe, S. Hishita, H. Kanda, Characterization of luminous-cubic boron-nitride single-crystals doped with Eu^{3+} and Tb^{3+} ions, Applied Physics Letters 87 (2005) 211913.
[14] B. He, W.J. Zhang, Y.S. Zou, Y.M. Chong, Q. Ye, A.L. Ji, Y. Yang, I. Bello, S.T. Lee, G.H. Chen, Electrical properties of Be-implanted polycrystalline cubic boron nitride films, Applied Physics Letters 92 (2008) 102103–102108.
[15] K. Nose, H. Oba, T. Yoshida, Electric conductivity of boron nitride thin films enhanced by in situ doping of zinc, Applied Physics Letters 89 (2006) 112123–112124.
[16] K. Nose, T. Yoshida, Semiconducting properties of zinc-doped cubic boron nitride thin films, Journal of Applied Physics 102 (2007) 063711–063715.
[17] K. Kojima, K. Nose, M. Kambara, T. Yoshida, Effects of magnesium doping on growth and electric conductivity of nanocrystalline cubic boron nitride thin films, Journal of Physics D: Applied Physics 42 (2009) 055304.
[18] J. Ying, X.W. Zhang, Z.G. Yin, H.R. Tan, S.G. Zhang, Y.M. Fan, Electrical transport properties of the Si-doped cubic boron nitride thin films prepared by in situ cosputtering, Journal of Applied Physics 109 (2011) 023715–023716.
[19] V.A. Gubanov, Z.W. Lu, B.M. Klein, C.Y. Fong, Electronic structure of defects and impurities in III–V nitrides: vacancies in cubic boron nitride, Physical Review B 53 (1996) 4377–4385.
[20] V.A. Gubanov, E.A. Pentaleri, C.Y. Fong, B.M. Klein, Electronic structure of defects and impurities in III–V nitrides. II. Be, Mg, and Si in cubic boron nitride, Physical Review B 56 (1997) 13077–13086.
[21] C.G. Van de Walle, J. Neugebauer, First-principles calculations for defects and impurities: applications to III-nitrides, Journal of Applied Physics 95 (2004) 3851–3879.
[22] S.J. Clark, M.D. Segall, C.J. Pickard, P.J. Hasnip, M.I.J. Probert, K. Refson, M.C. Payne, First principles methods using CASTEP, Zeitschrift fur Kristallograhie 220 (2005) 567–570.
[23] D.M. Ceperley, B.J. Alder, Ground state of the electron gas by a stochastic method, Physical Review Letters 45 (1980) 566–569.
[24] J.P. Perdew, A. Zunger, Self-interaction correction to density-functional approximations for many-electron systems, Physical Review B 23 (1981) 5048–5079.
[25] A. Janotti, D. Segev, C.G. Van de Walle, Effects of cation d states on the structural and electronic properties of III-nitride and II-oxide wide-band-gap semiconductors, Physical Review B 74 (2006) 045202.
[26] K. Laaksonen, M.G. Ganchenkova, R.M. Nieminen, Vacancies in wurtzite GaN and AlN, Journal of Physics: Condensed Matter 21 (2009) 015803.
[27] C.B. Samantaray, R.N. Singh, Review of synthesis and properties of cubic boron nitride (c-BN) thin films, International Materials Reviews 50 (2005) 313–344.
[28] H.S. Yang, N. Kurebayashi, T. Yoshida, in: T. Chandra, N. Wanderka, W. Reimers, M. Ionescu (Eds.), In situ S-doping of Cubic Boron Nitride Thin Films by Plasma Enhanced Chemical Vapor Deposition, Trans Tech Publ, Berlin, 2010, pp. 2956–2961.
[29] Y.-N. Xu, W.Y. Ching, Calculation of ground-state and optical properties of boron nitrides in the hexagonal, cubic, and wurtzite structures, Physical Review B 4 (1991) 7787–7798.